

Ab initio van der Waals interactions in simulations of water alter structure from mainly tetrahedral to high-density-like

Andreas Møgelhøj^{a,d}, André Kelkkanen^{a,b}, K. Thor Wikfeldt^c, Jakob Schiøtz^a, Jens Jørgen Mortensen^a, Lars G.M. Pettersson^c, Bengt I. Lundqvist^{a,b}, Karsten W. Jacobsen^a, Anders Nilsson^d and Jens K. Nørskov^{a,e,f}

^aCenter for Atomic-scale Materials Design (CAMD),

Department of Physics, Building 307, Nano DTU,

Technical University of Denmark, DK-2800 Kgs. Lyngby, Denmark

^bDepartment of Applied Physics, Chalmers University of Technology SE-412 96 Göteborg, Sweden

^cDepartment of Physics, Stockholm University, SE-106 91 Stockholm, Sweden

^dStanford Synchrotron Radiation Lightsource, 2575 Sand Hill Road, Menlo Park, California 94025, USA

^eSLAC National Accelerator Laboratory, 2575 Sand Hill Road, Menlo Park, California 94025, USA and

^fDepartment of Chemical Engineering, Stanford University, Stanford, CA 94305, USA

(Dated: March 17, 2019)

The structure of liquid water at ambient conditions is studied in *ab initio* molecular dynamics simulations using van der Waals (vdW) density-functional theory, *i.e.* using the new exchange-correlation functionals optPBE-vdW and vdW-DF2. Inclusion of the more isotropic vdW interactions counteracts highly directional hydrogen-bonds, which are enhanced by standard functionals. This brings about a softening of the microscopic structure of water, as seen from the broadening of angular distribution functions and, in particular, from the much lower and broader first peak in the oxygen-oxygen pair-correlation function (PCF), indicating loss of structure in the outer solvation shells. In combination with softer non-local correlation terms, as in the new parameterization of vdW-DF, inclusion of vdW interactions is shown to shift the balance of resulting structures from open tetrahedral to more close-packed. The resulting O-O PCF shows some resemblance with experiment for high-density water (A. K. Soper and M. A. Ricci, Phys. Rev. Lett., 84:2881, 2000), but not directly with experiment for ambient water. However, an O-O PCF consisting of a linear combination of 70% from vdW-DF2 and 30% from experiment on low-density liquid water reproduces near-quantitatively the experimental O-O PCF for ambient water, indicating consistency with a two-liquid model with fluctuations between high- and low-density regions.

I. INTRODUCTION

Liquid water plays a crucial role in all biological and numerous chemical processes which has been the incentive for many detailed experimental and theoretical studies probing both structural and dynamical properties of the fluid. However, the microscopic structure of ambient liquid water is still a matter of recent debate.^{1–23} In particular two classes of models are currently being considered, where the traditional model of water is based on a continuous distribution of distorted tetrahedral structures. This is typical of what most molecular dynamics simulations currently give. However, most of these simulations give over-structured O-O and O-H pair-correlation functions (PCFs) and show discrepancies in comparison to x-ray and neutron scattering experimental data.^{10,14} It is, however, possible to generate a more distorted tetrahedral structure model that is consistent with the diffraction data, but equivalent agreement is seen also for alternative asymmetrical and mixture models illustrating that diffraction data do not discriminate between differently hydrogen-bonded structure models.^{10,14,24} Based on recent findings correlating x-ray emission spectroscopy (XES) with x-ray Raman scattering (XRS) and small angle x-ray scattering (SAXS) data,¹⁵ a model has been suggested where a division into contributions from two classes of local instantaneous hydrogen-bonded structures is driven by incommensu-

rate requirements for minimizing enthalpy and maximizing entropy; in particular the XES data shows two well-separated peaks, which interconvert with changes in temperature.^{12,15,19} In the proposed picture the dominating class consists of a continuum of structures with some resemblance to high-pressure water,¹⁵ but with a further expanded first shell (more distorted H-bonds) and more disorder in the 2nd shell; this was based on the temperature dependent shift of the dominating peak in the XES spectra indicating more thermal distortion and disorder with increasing temperature. The second class corresponds to fluctuations where regions of strongly tetrahedral structures (similar to low-density water) appear in different sizes and shapes with a mean size interpreted from the SAXS data as $\sim 1\text{nm}$,¹⁵ but naturally many sizes and shapes would appear. It should be emphasized that since these are fluctuations no strict boundaries between the two classes should be expected. The attosecond (XRS, SAXS) to femtosecond (XES) time scales of the experimental probes are too fast for molecular motion to be followed and the experimental data thus correspond to a statistical sampling of instantaneous, frozen local structures in the liquid; no experimental information on the time-scale of such fluctuations is thus currently available.¹⁵ Besides being consistent with both neutron and x-ray scattering,¹⁴ this picture was recently also shown to bring a consistency between x-ray scattering and extended x-ray absorption fine structure (EXAFS) data, requiring both a fraction of straight, strong hydrogen-

bonds and disordered structures.²⁵ However, other opinions exist regarding the interpretation of SAXS, XES and XRS.^{2,8,11,17,18,20–23}

Most simple rare gas solids and liquids have a nearest-neighbor coordination of 12 whereas hexagonal ice, due to the directional H-bonds has a coordination of only 4. The latter leads to large open spaces in the ice lattice and low density. The dispersion, or vdW force, in condensed rare gases leads to non-directional, isotropic interactions. Similarly the inclusion of vdW interactions in *ab initio* simulations of water may counteract the directional interactions and lead to better agreement with, *e.g.*, experimental PCFs where it should be understood that, while this could be regarded as a minimum requirement of a water model, it is by no means sufficient for a complete description. Interestingly, it has been argued on thermodynamic grounds that over a large range of the liquid-vapor coexistence line the averaged water interaction potential should resemble that of liquid Argon.²⁶

Water shows many anomalies in its thermodynamic properties, such as compressibility, density variation and heat capacity.^{27,28} In attempts to explain this, directional H-bonds and more isotropic vdW forces are key concepts. While vdW forces are well defined as results of non-local electronic correlations, there is no unique way to characterize H-bonds in terms of topology or interaction strength. And yet "the H-bond governs the overall structure and the dynamics of water".²⁹ One of the models to explain the enhanced anomalies in supercooled water is the liquid-liquid critical-point (LLCP) hypothesis,^{30–32} with the most substantial role played by cooperative H-bond interactions among the water molecules.³³ The LLCP model explains the significant increase in density fluctuations upon supercooling water, which is evidenced by the anomalously increasing isothermal compressibility,³⁴ as resulting from the local formation of open tetrahedrally coordinated H-bond regions. It furthermore connects the deeply supercooled liquid state of water to the polyamorphism seen in ices, *i.e.* the distinct low-density and high-density amorphous ice phases (LDA/HDA). A high-density liquid (HDL) phase transforms to an ordered low-density phase (LDL) in the deeply supercooled region, through a first-order phase transition at high pressures above the LLCP and through a continuous smooth transition upon crossing the Widom line at ambient pressure.^{32,35–38} There are differences in their respective local structures; in pure HDL the local tetrahedrally coordinated H-bond structure is perturbed by a partially collapsed second coordination shell, while in the LDL a more open and locally "bulk-ice-like" H-bond network is realized.^{16,35}

The combined XES, XAS and SAXS results described above,¹⁵ which indicated nanoscale density and structural fluctuations, can be easily interpreted as reflections of this "competition" between the two local forms, HDL (maximizing entropy) and LDL (minimizing enthalpy) and thus viewed as extending an established picture of supercooled water into the ambient regime. Whether

HDL and LDL can exist as pure phases, accompanied by a liquid-liquid phase transition and a critical point, is still unresolved and alternative models, *e.g.*, singularity-free (SF),^{31,39} the critical-point-free (CPF)⁴⁰ and stability limit (SL) conjecture⁴¹ scenarios have been proposed, however still building on structural HDL/LDL fluctuations.

In the quantitative characterization of water, computer simulations play a vital role. Empirical force fields are frequently applied but with a questionable transferability since force fields are parameterized against experimental data or against a limited set of quantum chemically computed structures. Furthermore, many-body interactions beyond pair-interactions are frequently not taken into account. These deficiencies are eliminated in Car-Parrinello⁴² (CP) and Born-Oppenheimer (BO) molecular dynamics (MD), collectively known as *ab initio* (AI) MD. In AIMD, the forces are calculated using a first-principles electronic structure method, typically based on density functional theory (DFT). BOMD, used in the present study, minimizes the Kohn-Sham energy functional at each time step, keeping the nuclear positions frozen. In nearly all force field and *ab initio* molecular dynamics (MD) simulations of water at ambient conditions there seems to be a strong driving force to form highly directional hydrogen bonds (H-bond) leading to tetrahedral structures that are in general over-structured in terms of the derived PCFs. One exception is the coarse-grained mW water model⁴³ which has two terms in the interaction potential corresponding to anisotropic tetrahedral interactions and isotropic van der Waals (vdW) interactions, respectively, and which gives a maximum peak height of 2.3 in the O-O PCF at room temperature, in close agreement with recent analyses of experimental diffraction results.^{10,14,44–46} This model was shown to feature fluctuations between tetrahedral and disordered species resulting in a liquid-liquid transition in the supercooled region.⁴⁷ Empirical force-field models which have over-structured PCFs in agreement with older determinations^{48,49} have however also been shown to exhibit liquid-liquid phase transitions in the supercooled regime, *e.g.*, Refs. 32,50 and 51, indicating that the PCFs are not decisive for general trends in the thermodynamic behavior in water simulations.

Until recently, AIMD simulations of water have almost exclusively been performed with the BLYP⁵² and PBE⁵³ exchange-correlation (XC) functionals. However, these functionals are shown to significantly over-structure liquid water,⁵⁴ as seen from the maximum value and sharpness of the first peak in the oxygen-oxygen PCF.^{10,14,44–46,55,56} AIMD simulations of water have furthermore been shown to depend on which functional is applied and to give different predictions for different XC functionals.⁵⁷ MD simulations performed using generalized gradient approximations (GGA) tend to over-structure liquid water and lead to diffusion constants two to three times too small compared to experiment; using hybrid functionals only marginally improves the

results.⁵⁸ In addition, it has been shown that PBE-based AIMD simulations lead to a melting point of ice at 417 K and therefore simulations at ambient conditions with this functional will describe a deeply supercooled state which is over-structured with respect to real liquid water at ambient conditions.⁵⁹ As we will show in the following, inclusion of the more isotropic vdW interaction balances the directional forces allowing a partial break-down of the H-bond network and a much less structured liquid.

II. METHODS

A. Role of van der Waals forces

Small water clusters have been studied using the PBE and BLYP XC functionals, which do not explicitly include van der Waals (vdW) interactions, and the results compared to high accuracy methods such as coupled cluster (CCSD(T)) and Møller-Plesset (MP2). Near chemical accuracy for the strength of the H-bond for the water dimer is obtained using PBE⁶⁰ while BLYP consistently underbinds small water clusters.⁶¹ However, discrepancies arise and increase with the size of the water cluster for both PBE and BLYP which has been ascribed to the lack of a description of vdW forces.⁶¹ One could thus argue that obtaining the correct result for the water dimer is no guarantee for a correct description since not all physical interactions relevant for larger clusters are sampled by the dimer.

While it is well established that H-bonds give the major contributing factor to the dynamics and structure of water, vdW interactions have also been suggested to be important^{62,63} and, in line with this, thermodynamic considerations have led to the suggestion that the averaged water interaction potential should resemble that of liquid Argon.²⁶ The angular dependence of the H-bond is anticipated to have a big impact on the PCF and self-diffusion coefficient.⁶⁴ If, for example, it is too difficult to bend a DFT H-bond, the diffusion coefficient should come out too small, which it does. Many other suggestions to explain the too small diffusion coefficient exist however⁶⁴ but balancing the directional H-bond interactions with more isotropic vdW forces would intuitively contribute to softening the H-bond network and allow more efficient diffusion. Traditional local and semi-local DFT do not, however, contain non-local vdW interactions, *e.g.*, BLYP being especially incapable of describing dispersion.⁶⁵ Influences of vdW interactions have been investigated using MD based on empirical potentials,^{62,66} *e.g.*, performed with a dispersion-corrected BLYP XC functional,⁶⁷ or using empirically damped C_6R^{-6} corrections⁶⁸⁻⁷⁰ to describe the vdW interactions.

A way to introduce vdW forces in DFT from first principles is provided by the van der Waals density functional vdW-DF,⁷¹ recently used for the first time in AIMD on liquid water.⁷² The inclusion of vdW forces using the vdW-DF was shown to greatly improve water's equilib-

rium density and diffusivity. However the vdW-DF MD also produces a collapsed second coordination shell giving rise to new structural problems that have been suggested to depend partially on the choice of exchange used in the vdW functional.⁷²

The vdW-DF method proposed by Dion *et al.*⁷¹ accounts for exchange by an exchange functional that gives Hartree-Fock-like repulsion at relevant separations and that includes non-local correlation, and thus vdW forces, by calculating the dielectric response in a plasmon-pole approximation. It gives the correct stability trend for low-lying water hexamers⁷³ but returns a significant underbinding for most H-bonds.⁷³⁻⁷⁵ The underbinding can be remedied by using an exchange functional that gives more binding⁷⁶ at typical H-bond separations,^{73,74,77} like the PW86,⁷⁸ optPBE,⁷⁹ and C09⁸⁰ exchange functionals. Recently Klimes *et al.*⁷⁹ proposed a new vdW density functional, optPBE-vdW, based on the original vdW-DF functional.⁷¹ This scheme shows promise in the description of dispersion and H-bond systems, as it reduces the underbinding given by the vdW-DF down to chemical accuracy while preserving the correct hexamer trends. However, this improved behavior is obtained at the cost of poorer performance on the binding energy of small molecules.⁸¹ Very recently a second version of the vdW-DF, called vdW-DF2, was suggested,⁸² using a new non-local correlation functional along with PW86 as an appropriate exchange functional. Both optPBE-vdW and vdW-DF2 give chemical accuracy on the water dimer, albeit with slightly different non-local-correlation and exchange functionals. In the present study we therefore wish to investigate the microscopic structure of liquid water by performing AIMD using both the new optPBE-vdW and vdW-DF2 XC functionals to also investigate the importance of the balance between correlation and exchange in liquid water AIMD simulations.

B. The optPBE-vdW and vdW-DF2 exchange-correlation functionals

In general a vdW-DF functional takes the form

$$E_{xc} = E_x^{\text{GGA}} + E_c^{\text{LDA}} + E_c^{\text{nl}}, \quad (1)$$

where E_x^{GGA} is an exchange functional using the generalized gradient approximation (GGA), E_c^{LDA} accounts for the local correlation energy by using the local density approximation (LDA). LDA is chosen to avoid double counting of correlation. The non-local correlation energy describing the vdW interaction is given by the six-dimensional integral⁷¹

$$E_c^{\text{nl}} = \frac{1}{2} \int \int n(\mathbf{r}) \phi(\mathbf{r}, \mathbf{r}') n(\mathbf{r}') d\mathbf{r} d\mathbf{r}', \quad (2)$$

where $\phi(\mathbf{r}, \mathbf{r}')$ is the interaction kernel and depends on the density and its gradient. The non-local term is calculated as suggested in Ref. 83. In the original vdW-DF from

Dion *et al.* the exchange functional from revPBE⁸⁴ is utilized.

The optPBE-vdW functional is constructed like vdW-DF⁷¹ but uses an alternative exchange functional. The latter takes the same form as both the PBE and RPBE exchange, but the parameters of the exchange enhancement factor are optimized against the S22 database.⁷⁹ The S22 database⁸⁵ is a set of 22 weakly interacting dimers, mostly of biological importance, including the water dimer.

The vdW-DF2⁸² has the form of Eq. (1) and uses the PW86 exchange,⁸⁶ which is argued in Ref. 77 to give the most consistent agreement with Hartree-Fock (HF) exact exchange, and with no spurious exchange binding. Furthermore, a new approximation for E_c^{nl} is used to calculate the value of the interaction kernel in Eq. (2).⁸² This new functional has been shown to give very accurate results for the water dimer as compared to benchmark CCSD(T) calculations^{82,87} and to compare closely to the present S22 benchmark.⁸⁸

C. Computational protocol

Ab initio molecular dynamics simulations are performed in the NVE ensemble with optPBE-vdW, vdW-DF2, and PBE, using the grid-based real-space projector augmented wave code, GPAW.^{89,90} A wave function grid spacing of 0.18 Å and Fermi smearing with a width of 0.01 eV have been used. The grid spacing has been determined by comparing DFT calculations of water hexamers with CCSD(T) results. In the electronic structure calculations a strict energy convergence criterion of 10^{-7} eV per electron is used in order to determine the forces adequately.

All internal bond lengths are kept fixed at 0.9572 Å (an MP2 optimized gas phase geometry obtained from the G2-database)⁹¹ but angles are allowed to vary (*i.e.* bending vibrations are included); eliminating the high-frequency OH-stretch allows longer time steps in the simulations. In the initial configuration 64 water molecules are placed in a simple cubic lattice with random orientations in a cubic periodic box with side lengths 12.42 Å, to reproduce a water density of 1 g/cm³. The geometry is then optimized to obtain a configuration at zero Kelvin (using PBE), from which the MD is started giving the atoms random velocities according to a Maxwell-Boltzmann velocity distribution corresponding to two times 300K, keeping the center of mass of the box stationary. Approximately half of the kinetic energy converts to potential energy thus giving an average temperature around 300K. An initial equilibration of 10 ps using the PBE XC functional is performed followed by 2.5 ps vdW equilibration of the simulations using optPBE-vdW and vdW-DF2. For all methods equilibration was followed by production runs for 10 ps which is the minimum time reported necessary due to the slow diffusion of water.⁹² Using 64 water molecules has been shown to be adequate

to remove the most significant problems concerning finite size effects⁹³ and is feasible within the current computational capabilities. The Verlet algorithm is employed using a time step of 2 fs in the NVE ensemble. Using this type of ensemble the temperature is allowed to fluctuate and the average temperature of the PBE, vdW-DF2 and optPBE-vdW simulations were 299K, 283K and 276K, respectively.

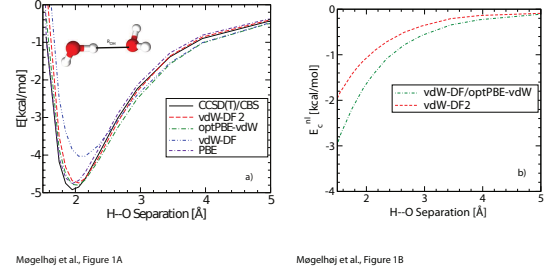


FIG. 1: a) The water dimer potential energy curves calculated with DFT using the XC functionals PBE, vdW-DF, vdW-DF2 and optPBE-vdW, respectively, are compared to CCSD(T)/CBS wave function results.⁸⁷ b) The distance dependence of the non-local contribution (Eq. (2)) to the interaction energy of the water dimer for the XC functionals vdW-DF2 and optPBE-vdW, shows that, when they give similar potential energies (Fig. 1a)) they do so for different reasons; the optPBE-vdW gets more binding from a stronger vdW attraction but vdW-DF2 gets more net attraction from a less repulsive exchange.

III. RESULTS

A. Water dimer

Before discussing the MD results we compare the functionals for a simpler but still relevant system: the water dimer. Fig. 1 a) illustrates the potential energy curve for the water dimer calculated using PBE, vdW-DF, vdW-DF2 and optPBE-vdW in comparison with the benchmark CCSD(T) curve from Ref. 87. Fig. 1 a) shows that the vdW functionals are capable of describing this basic constituent of liquid water extremely accurately, however for different reasons. The non-local contribution (E_c^{nl}) to the dimer binding from the two functionals is plotted in Fig. 1 b). The non-local part of the optPBE-vdW functional, which is based on the older approximation, is more attractive as mentioned in Ref. 82. Since less attraction stems from the non-local interaction in the vdW-DF2, while the total energy for the dimer is almost identical to that of optPBE-vdW, the remaining part of the interaction energy must give a larger contribution for the vdW-DF2 than for optPBE-vdW. The remaining part of the interaction energy includes electrostatic interaction, electronic correlation, and more or less repulsive exchange. Since electrostatic interactions only depend

on separation, and local correlation is treated identically with the LDA correlation in both cases, this difference has to come from the different choices for the exchange. The PW86 exchange in vdW-DF2 is hence less repulsive than the optPBE exchange in optPBE-vdW; a possible cause of the reported collapsed second-shell structure was in Ref. 72 suggested to be that the non-local parameterization of exchange used in vdW-DF and optPBE-vdW may be too attractive when used in MD. This is, however, not the case, as seen from the pair-correlation functions (PCFs), to be discussed next.

B. Pair-correlation functions

Fig. 2 a) illustrates that AIMD simulations of liquid water using vdW-DF2 and optPBE-vdW give very similar O-O PCFs which are, however, very different from the O-O PCF from PBE and furthermore from those derived from experiment using either Empirical Potential Structure Refinement (EPSR)⁴⁴ or Reverse Monte Carlo (RMC)⁹⁴ to fit the structure factor.^{10,14} In the simulations both functionals result in the same characteristics as reported in Ref. 72, including a lower first peak shifted to larger O-O separation than for normal GGAs as well as for experiment on ambient water. The second coordination shell at 4.5 Å is also completely smeared out where correlations from the region 4-5 Å have instead moved into the region 3.3-3.7 Å. The non-local correlation differences in the functionals do not, however, result in significantly different O-O PCFs. In contrast, the very recent vdW-DF MD simulation showed that by changing the exchange in vdW-DF from revPBE to PBE, the second shell structure again became well defined.⁷² However, the exchange functionals of revPBE and PBE are quite different, and the potential of the dimer is not reproduced very well using the PBE exchange with LDA and non-local correlation.

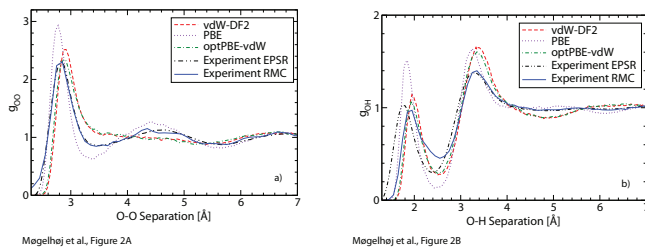


FIG. 2: a) Oxygen-oxygen PCFs (g_{OO}) obtained from experimental data using EPSR⁴⁴ and RMC¹⁴ in comparison with PCFs obtained by DFT MD simulations using PBE, optPBE-vdW and vdW-DF2. b) Oxygen-hydrogen PCFs (g_{OH}) obtained from experimental data using EPSR⁴⁴ and RMC¹⁴ in comparison with PCFs from PBE, optPBE-vdW and vdW-DF2.

Compared to the experimentally derived O-O PCFs it is clear that the PCF obtained from PBE is severely over-

structured while the simulations including vdW forces have resulted in a structure significantly less structured than what is experimentally observed for ambient liquid water. We will return to this point in the discussion section below.

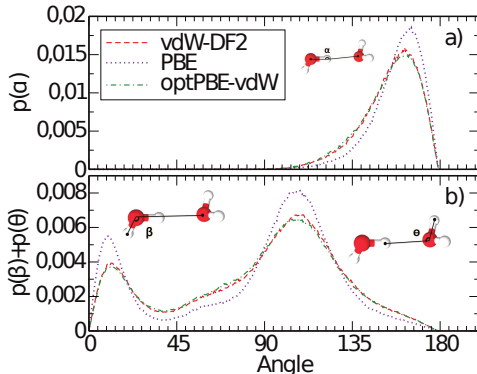
Some discrepancy in the O-H PCF function for the vdW XC functionals compared to experiment is seen in Fig. 2 b), which we shall now discuss. The O-O correlations can be obtained from a Fourier transform of the x-ray diffraction data, if a large enough Q-range has been measured and the data can be properly normalized; x-ray scattering is strongly dominated by the electron-rich oxygens. Neutron diffraction data, on the other hand, contain simultaneous information on the H-H, O-H and to some extent, the O-O PCFs, making a direct Fourier transform to extract a specific PCF inapplicable. Various fitting schemes of structure models to the experimental structure factors have therefore been developed, and we show two such fits to the same experimental data using the EPSR⁴⁴ and RMC method¹⁴, respectively.

There is a significant difference in the first peak position in the O-H PCF between the two methods compared to what is found for the O-O PCF. This can be understood from the relatively lower sensitivity of the neutron data to specifically the O-H correlation in comparison to the sensitivity of x-ray data to the O-O correlation.¹⁴ The EPSR technique uses the assumed reference pair-potential to provide structural aspects not included in the experimental data,^{14,24} while structural aspects not determined by the experimental data, or imposed constraints, will in the RMC technique simply result in a phase-space weighted sampling of structures consistent with the experimental structure factors;⁹⁵ combining the two methods thus gives additional information on the uncertainties and assumptions in the resulting fits. It is interesting to note that the RMC method gives a shift in the first peak of the O-H correlation out to nearly 2 Å,¹⁴ which agrees well with the vdW MD simulations presented here, while the EPSR solution is closer in position to the PBE, likely reflecting the starting potential in the EPSR fitting procedure. Note, that both the RMC and EPSR fits reproduce the experimental scattering data equally well, implying that the position of the first intermolecular OH correlation is not strictly determined by the data, leaving an uncertainty in the diffraction-derived PCFs.^{14,96} The first peak in the PBE O-H PCF is clearly too high and the first minimum at 2.5 Å too low, however, while all three simulations exaggerate the height of the second peak at 3.2 - 3.6 Å.

C. Angular distribution functions and hydrogen-bonding analysis

That the van der Waals functionals provide a smoother angular structure with less tetrahedral bonding can be demonstrated by considering the angular distribution functions and the average number of H-bonds per wa-

ter molecule. The cone criterion from Ref. 1 has been applied as a geometric H-bond definition: $r_{OO} < r_{OO}^{\max} - 0.00044\delta_{\text{HOO}}^2$, which defines a cone around each H-bond-donating OH group, where $r_{OO}^{\max} = 3.3$ Å is the maximum OO distance at zero angle δ_{HOO} , where δ_{HOO} is the H-O...O angle quantifying the angular distortion of the H-bond. Table I shows the H-bond statistics for PBE, optPBE-vdW and vdW-DF2. PBE is seen to prefer a tetrahedral structure with a majority of the molecules having 4 H-bonds. With its relatively more repulsive exchange optPBE-vdW gives its water molecules less incentive to choose a fully H-bonded structure, resulting in a larger amount of water molecules having two or three H-bonds. The vdW-DF2 comes in between with its relatively weaker vdW interaction giving slightly higher preference to forming H-bonds. This analysis suggests that there is a competition between isotropic vdW forces and directional H-bonds, resulting in fewer or more H-bonds per water molecule depending on the applied approximations; however, between the vdW models the average number of H-bonds varies only weakly despite differences in vdW strength.



Møgelhøj et al., Figure 3

FIG. 3: Molecular angular distributions in liquid water according to MD simulations using DFT with the indicated functional. a) The angular distribution functions of the O-H...O angle. b) the H-O...O (first peak) and $\theta = \angle \text{H}\cdots\text{O}-\text{H}$ (second peak) angles obtained using the XC functionals PBE (yellow), vdW-DF2 (red) and optPBE-vdW (green). When including vdW interactions a softening of the structure is seen from the broader distribution of angles.

We note in particular the low number of double-donor, double-acceptor tetrahedral molecules according to the cone criterion¹ for the two vdW models. In fact, the large number of broken H-bonds in the vdW simulations suggests that these models are in closer agreement with predictions from x-ray spectroscopies^{1,12,15,97} compared to most other AIMD models and future calculated x-ray spectra based on optPBE-vdW and vdW-DF2 structures will provide an interesting opportunity to obtain further insight regarding the interpretation of these spectra.

No. H-bonds \ Method	PBE	optPBE-vdW	vdW-DF2
1	2	10	8
2	12	29	27
3	31	37	38
4	52	22	25
5	3	1	1

TABLE I: Percentage distribution of hydrogen bonds per water molecule calculated using the cone criterion from Ref. 1. PBE results are shown to favor more H-bonds compared to either vdW functional, which both allow for a larger number of molecules to break the tetrahedral structure with four bonds.

The angular distribution functions (ADFs) of the H-bonds are shown in Fig. 3. The ADFs of H-bond acceptor and donor give information on the orientational flexibility of the water molecules. In the ADFs only the angles between a central molecule and the molecules of the first solvation shell are considered by using a cutoff distance corresponding to the first minimum in the PBE O-O PCF; this distance was applied also to the vdW MDs where the second shell is smeared out and no minimum is visible. Fig. 3 a) displays the distributions of donor angles $\alpha = \angle \text{O}-\text{H}\cdots\text{O}$ for the various simulations. The first peak in Fig. 3 b) is β , the deviation of the O-H...O bond from being linear, which gives information on the flexibility of donor H-bonds while the second peak is the acceptor angle $\theta = \angle \text{H}\cdots\text{O}-\text{H}$. The distribution of angles has been found to depend on the choice of water model.⁹ The picture of a competition between non-directional vdW interactions and directed H-bonds seems to be supported by the ADFs as illustrated by the fact that the model without vdW forces (PBE) has no incentive to deviate from a structure of strong H-bonds, thus resulting in a relatively straight H-bond angle. When including vdW forces the H-bonds become significantly more bent. In general a softening of the structure is seen from the broader ADFs obtained in case of the vdW-DFs.

D. Tetrahedrality and asphericity

Two useful measures of the local coordination of molecules in water are the tetrahedrality^{98,99} and asphericity¹⁰⁰ parameters. The former quantifies the degree of tetrahedrality in the nearest neighbor O-O-O angles and is defined as

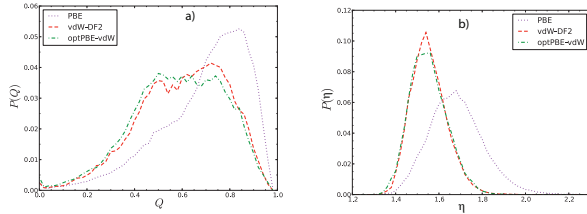
$$Q = 1 - \frac{3}{8} \sum_{i=1}^3 \sum_{j>i}^4 \left(\cos \theta_{i0j} + \frac{1}{3} \right)^2 \quad (3)$$

where θ_{i0j} is the angle formed by two neighboring oxygen atoms i and j and the central molecule 0. Only the four nearest neighbors are taken into account which makes Q a very local measure. Perfect hexagonal ice gives $Q = 1$ for all molecules while the ensemble average over an ideal gas gives $\langle Q \rangle = 0$.⁹⁹ The asphericity parameter is defined

as

$$\eta = \frac{A^3}{36\pi V^2} \quad (4)$$

where A and V are the area and volume of the Voronoi polyhedron of the molecule in question. Contrary to Q , η is sensitive also to interstitial molecules outside the first shell and to the second coordination shell since these add surfaces to the Voronoi polyhedron, making it more spherical. The two relevant limits for water are that of hexagonal ice, which gives $\eta = 2.25$, and that of a perfect sphere which gives $\eta = 1$; larger disorder in the local coordination thus gives smaller values of η .



Mogelhoj et al., Figure 4A

Mogelhoj et al., Figure 4B

FIG. 4: a) Distributions of the tetrahedrality parameter Q . vdW interactions lead to significantly lower average tetrahedrality and a strong low- Q peak from interstitial molecules around $Q = 0.5$. b) Distributions of the asphericity parameter η . A large effect of vdW interactions is seen with a shift towards more spherical (less ice-like) values.

As Fig. 4 shows, the inclusion of the vdW interaction has a dramatic effect on both the tetrahedrality and asphericity distributions. The PBE simulation displays a strong peak at $Q = 0.8$, signifying a dominance of locally tetrahedral O-O-O angles, while both vdW simulations show an attenuation and shift of the high- Q peak to lower tetrahedrality along with the appearance of a strong low- Q peak associated with interstitial molecules at non-tetrahedral positions in the first coordination shell. Out of the two vdW models, optPBE-vdW is seen to be somewhat less tetrahedral, consistent with their differences in H-bond statistics and PCFs discussed above. This is clearly illustrated by the average tetrahedrality which is 0.692, 0.602 and 0.583 for PBE, vdW-DF2 and optPBE-vdW, respectively. In comparison the average tetrahedrality has been estimated to be 0.576 using the EPSR method;¹⁰¹ note, however, that the tetrahedrality parameter is rather uncertain, *i.e.* the same diffraction data have been shown to support tetrahedrality values ranging from 0.488 to 0.603.¹⁴ An even larger difference is seen in the asphericity distributions; the two vdW models show sharper peaks centered at lower asphericity values compared to PBE. This directly reveals the large disorder in second-shell correlations in the vdW models, resulting from the tendency to form more isotropic local structures when vdW forces are included. Similarly to the comparison between the PCFs of the two vdW models discussed above, it can be seen

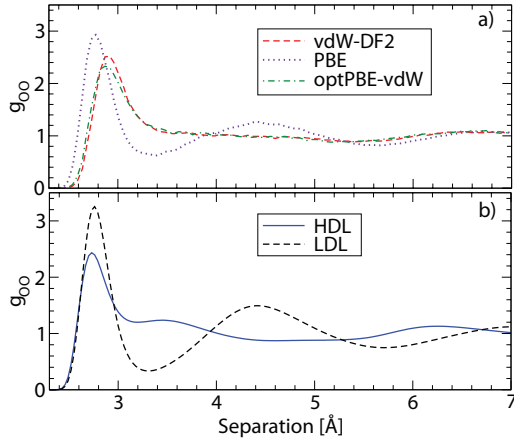
here that despite non-local differences between vdW-DF2 and optPBE-vdW their respective liquid water structures turn out to be rather comparable in terms of both first- and second-shell correlations. The average asphericity is 1.681, 1.552 and 1.552 for PBE, vdW-DF2 and optPBE-vdW, respectively.

IV. DISCUSSION

Comparison of the results from the simulations using PBE with those including the vdW interactions shows a strong shift in the balance between directional H-bonding and more isotropic interactions; the former leads to tetrahedral H-bond coordination and low density while the latter favors a more close-packed ordering and higher density as evidenced by the loss of distinction between first and second coordination shells and the reduced number of H-bonds in that case. Having two balancing interactions that favor opposite structural properties is a prerequisite for fluctuations; it is clear that by tuning either the importance of H-bonding or the vdW interaction the preference for either structure will be affected in the simulations. If we consider the proposed model of fluctuations between HDL and LDL,^{15,102} it could well be that the vdW models under the present conditions only generated an HDL-like structure while without including vdW the resulting structure is more LDL-like.

Computational resources only allow the 64 molecules to be followed for a time of up to about 10 ps. If the two proposed structures of liquid water truly coexist as endpoints of fluctuations in nanosized patches of different local density, as suggested in Ref. 15, then an AIMD with only 64 water molecules in a fixed volume may not be suitable to observe this behavior; a much larger box size or an NPT ensemble simulation allowing the box size to vary would be required. The relatively small simulation (12.42 Å box length) and short run time will only observe a local structure of water which, in this picture, is either approximating LDL- or HDL-like; LDL-like simulations can be performed with the PBE XC functional, which is known to give a local tetrahedrally coordinated H-bond structure, but to prefer a density significantly lower than for ambient water.⁷² It should be noted that the simulations are run in the NVE ensemble with density fixed to correspond to ambient conditions which, under the assumption that ambient water is dominated by HDL,^{1,12,15,103,104} should favor an HDL-like structure over fluctuations towards LDL, if energetically allowed, as seems to be the case with vdW interactions included.

The structure obtained with the vdW functionals is an important step towards an HDL-dominated liquid at ambient conditions as suggested should be the case by all studies of the phase diagram in the supercooled regime. The tendency towards an HDL-like liquid is seen by comparing the PCFs from MD simulations performed using the vdW-DF2 and optPBE-vdW XC functional (Fig. 5 a)), respectively, with the results of a neutron diffraction



Møgelhøj et al., Figure 5

FIG. 5: a) Oxygen-oxygen PCFs (g_{OO}) obtained by MD simulations from DFT with PBE, optPBE-vdW and vdW-DF2 functionals. b) Experimental PCFs for high- and low-density water.⁴⁸

study⁴⁸ where the LDL and HDL PCFs were extrapolated from data at different pressures; the resulting LDL and HDL PCFs are illustrated in Fig. 5 b). The EPSR derived HDL PCF is rather similar to the PCF obtained using a Fourier transform of x-ray diffraction data at high pressures¹⁰⁵ and furthermore seen to be very similar in terms of the second- and third-shell structure to that derived from vdW-DF2 and optPBE-vdW MD simulations; the effect of increasing pressure on the O-O PCF is that the 4.5 Å correlation disappears and moves to the 3.3 - 3.7 Å region and the third shell is shifted down to 6 Å.¹⁰⁵ The O-O PCFs obtained using the vdW functionals similarly show a lack of a well defined structure at 4.5 Å, an increase in correlations at 3.3-3.7 Å and show a shift towards shorter separations in comparison to PBE of the correlation at 6 - 6.5 Å, as is seen from Fig. 5. Both are clear indications towards HDL water. However, in contrast to the high pressure PCFs, a well defined peak at 3.5 Å is not present in the vdW MD simulations, but only an increase in correlations, and the first peak position is shifted outwards, which is not observed for pressurized water. It could be argued that a well-defined peak at 3.5 Å should not be expected since HDL-like water at ambient conditions should be thermally excited with a more expanded first shell and therefore further disordered in comparison to HDL water obtained under pressure.^{12,15} In particular, entropy effects due to high thermal excitations leading to higher disorder can be expected to create a structure, where both the first shell and, in particular, the collapsed second shell are distributed over a range of distances, leading to what is often denoted interstitial positions and with the first O-O peak appearing at longer distance when not under pressure. In this respect a comparison with the amorphous high-density (HDA) and very high-density (VHDA) ices is of interest, where for VHDA the second shell moves inwards and a peak at

3.4 Å develops while for HDA the second peak broadens significantly which indicates that various interstitial sites may be occupied making the high-density forms less well-defined.¹⁰⁶⁻¹¹⁰ It should be mentioned that a peak at ~ 3.7 Å is present in the MD simulation performed by Wang *et al.*⁷² using the earlier vdW-DF⁷¹ formulation of the functional.

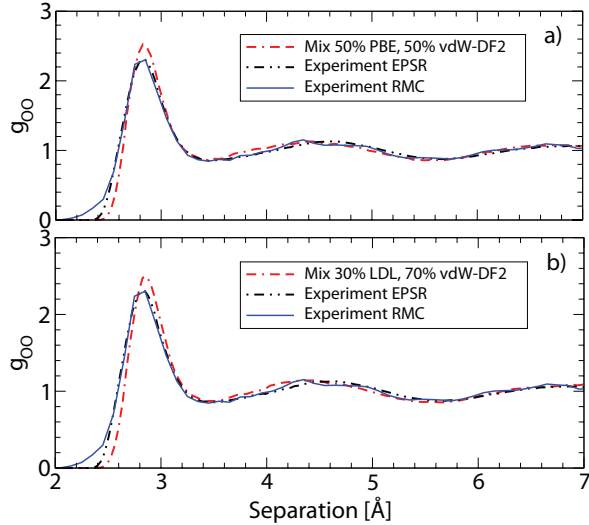
A minimum prerequisite for the hypothesis of fluctuations in the real liquid between HDL and LDL-like local structures is that the O-O PCF can be reproduced in such a picture while keeping in mind that reproducing the details of the O-O PCF does not guarantee a good description in other respects. However, it does provide a significant base-line that should be attained by any model of liquid water. The PCFs are, however, not directly measurable but derived from experimental data and we first need to discuss specifically the choice of O-O PCF for the comparison.

X-ray and neutron diffraction data treated in conjunction, either by the technique of empirical-potential structure refinement (EPSR)⁴⁴ or by reverse Monte Carlo (RMC) simulations,^{10,14} as well as from directly Fourier transforming the latest high-quality x-ray diffraction data sets,^{45,46} give a broad and slightly asymmetric first O-O peak with height 2.1-2.3 which is significantly lower than from standard MD simulations (height ~ 3) and from previous analyses of either only neutron diffraction data using EPSR⁴⁸ or analysis of the total x-ray scattering $I(Q)$ in terms of comparison to computed $I(Q)$ from MD simulations.⁴⁹

There were, however, problems with both the latter approaches^{48,49} since neutron diffraction mainly measures H-H and O-H correlations and thus contain insufficient data to modify the initial MD force-field guess in EPSR to a solution that also describes the O-O PCF, which is mainly determined by x-ray diffraction. The assumption by Hura *et al.*⁴⁹ was that some existing MD force-field should describe the total $I(Q)$; the best agreement was found for the TIP4P-pol2 potential from which pair-correlation functions were subsequently extracted. However, the internal molecular scattering strongly dominates $I(Q)$ in x-ray scattering and masks the more relevant intermolecular scattering such that small, but significant discrepancies in phase and amplitude at higher Q ,¹⁰ which determine the shape and height of the first O-O peak, were not observed and taken into account. Since the two independent studies based on, respectively, neutron and x-ray diffraction data arrived simultaneously at similar peak height and shape this was understandably taken as proof that the O-O PCF had been determined correctly; however, both studies reproduced in a sense the force-field used for the analysis and neither was strictly correct.

This state of affairs was analyzed more deeply in subsequent work by Soper, who in two seminal papers^{24,44} first showed that diffraction data do not contain enough information to discriminate between structure models of strongly different H-bond topology and then that a com-

combination of x-ray (sensitive to O-O and O-H correlations) and neutron diffraction data (sensitive to O-H and H-H correlations) is required to obtain reliable estimates of the three PCFs. Considering the significantly reduced height of the first O-O peak it was concluded that softer MD potentials were called for;⁴⁴ similar conclusions were reached based on RMC fits to the same data sets.^{10,14}



Møgelhøj et al., Figure 6

FIG. 6: a) Oxygen-oxygen PCFs based on mixing the vdW-DF2 and PBE structures. b) Mixing of experimental LDL and vdW-DF2 oxygen-oxygen PCFs in comparison with PCFs from reverse Monte Carlo (RMC)¹⁴ and EPSR analyses (EPSR) of experimental data.⁴⁴

We now test whether the obtained O-O PCF from the vdW models, with their low and asymmetric first peak at long distance and smeared out second shell, can be compatible with the PCF for ambient water by weighting together the vdW models with models of LDL to a combined PCF and comparing with the PCF derived from experiment using EPSR⁴⁴ and RMC.¹⁴ We have used two approximations of the LDL contribution. Since the PBE model gives severe over-structuring we can assume that it describes the low-density tetrahedral water structure (LDL), albeit not at its preferred density.⁷² In Fig. 6 a) the O-O PCF is plotted using a mixture of PBE and vdW-DF2 PCFs. This suggests that a 1:1 mixture of HDL (vdW-DF2) and LDL (PBE) could be compatible with the experimental O-O PCF. However, since the PBE simulated structure is far from its preferred density,⁷² it can be assumed to have too large distortions from the "real" LDL, and we therefore also compare with the experimental LDL PCF from Soper and Ricci.¹¹¹ In fitting to the experimental O-O PCF we obtain an equivalent agreement (Fig. 6 b)) with a 70:30 mixture between vdW-DF2 HDL PCF and the experimentally derived LDL PCF.¹¹¹ This ratio is most interesting, since it is very close to the original estimate of Wernet *et al.*¹ and the estimation based on x-ray emission spectroscopy,^{12,15}

as well as to that from interpreting infrared data in connection with analysis of a fractional Stokes-Einstein relation in water.¹⁰⁴ Note furthermore, that quantum effects have not been included in the simulations which would be expected to bring down and broaden the first O-O correlation additionally.^{112,113}

As has been pointed out by Soper²³ when combining two separate PCFs one must also consider whether the combination introduces additional cross-terms between the two, *i.e.* that the contribution to the total PCF from considering pairs of atoms, one from each distribution, could change the picture. This would be expected from a combination of two highly structured PCFs with well-defined peaks occurring at different interparticle separations in the two distributions. However, considering that both the LDL and HDL local structures give a peak in the region of 2.7 - 3 Å and beyond that the HDL-like PCF is basically without structure it seems likely that in this particular case no extra features should be expected from cross contributions to a combined PCF.

The question is naturally why the vdW simulation only shows the appearance of HDL-like water and why, in order to obtain agreement with x-ray diffraction experiments, it is necessary to artificially add an LDL component. One potential explanation could be related to the fact that the simulation is performed in the NVE ensemble which keeps the volume fixed and thus does not allow fluctuations of the density of the box and that this penalizes LDL to a greater extent than HDL once the more isotropic vdW interactions are included; the NVE ensemble is equivalent to adding a pressure to maintain the box size which would disfavor fluctuations to lower density assuming that the density at ambient conditions corresponds more closely to that of HDL. The box is furthermore rather limited with only 64 molecules. In order for spatially separated fluctuations between HDL and LDL to develop fully it might be necessary to use much larger simulation boxes, in particular if the fluctuations are of a mean length scale around 1 nm as suggested in Ref. 15. There is furthermore some experimental evidence from thin water films on slightly hydrophobic surfaces that only an HDL related structure is observed even in the supercooled regime,¹¹⁴ indicating that if the system size becomes very small, indeed only one class of local structure is observed and the formation of LDL-like local regions is suppressed.

V. CONCLUSIONS

The new van der Waals density functionals optPBE-vdW and vdW-DF2 show great promise in describing the basic structural constituents of liquid water, as seen from comparing calculations of water dimer and hexamers with benchmark coupled cluster CCSD(T) results.^{73,79,82} A softening of the structure of liquid water at ambient conditions is observed when including vdW interactions, consistent with previous work.^{67,72} This is seen

from the broader angular distributions, the more disordered tetrahedrality and asphericity distributions, and from the much lower and broader first peak of the oxygen-oxygen PCF obtained from the optPBE-vdW and vdW-DF2 models compared to PBE. The lower first peak of the O-O PCF improves the agreement with experiment significantly. However, the outer structure is washed out by the vdW forces. This has been suggested⁷² to be related to non-local correlations, but our study of functionals with different non-local correlation strength did not show any significant difference in the liquid structures, while both were found to be very accurate for the water dimer. Instead we find that the inclusion of the more isotropic vdW interaction shifts the balance over from directional H-bonding towards a more close-packed system, *i.e.* a competition between directional and isotropic interactions.

The vdW simulations seem to be potentially consistent with a picture of fluctuations between two different water structures instantaneously coexisting in nanoscale patches albeit not directly observing fluctuations except in the sense of obtaining two alternative endpoints with vdW forces included (HDL) or excluded (LDL). The relatively small simulation can only give a picture of the local structure of water, and while PBE predominantly describes an approximation to low-density water, both optPBE-vdW and vdW-DF2 tend to describe an approximation to high-density water. By comparing the O-O PCFs of the vdW models with PCFs from x-ray¹⁰⁵ and neutron⁴⁸ diffraction of water at different pressures we note a resemblance between the vdW models and high-density water in terms of effects on the second- and third-neighbor correlations while the expansion of the first coordination sphere found in the simulations may in experiments be counteracted by the pressure applied to generate pure HDL experimentally. The comparison to HDL is further supported by the reduction of the average number of H-bonds per molecule in the vdW MD simulations, which is a result of the isotropic vdW forces competing with the directional H-bond formation. Varying the

strength of the exchange interaction does not result in a significant change in number of bonds once the vdW interaction is included. A 1:1 mixture of PBE (LDL) and vdW-DF2 (HDL) structures is compatible with the latest x-ray O-O PCF, an equivalent agreement is achieved for a 70:30 mixture of vdW-DF2 and the experimentally determined LDL PCF.

The present work does not resolve the debate on water structure but it suggests for further investigation the van der Waals interaction as a physically sound mechanism which affects the balance between directional H-bonding and higher packing and may thus indicate a way to reconcile the interpretation of recent x-ray spectroscopic data with structures obtained from AIMD simulations of liquid water. It is likely that much larger and longer simulations in the NPT ensemble are needed to determine whether current vdW models support a temperature-dependent balance of fluctuations between HDL and LDL-like structures in ambient water, as suggested by recent x-ray spectroscopic and scattering results,¹⁵ and which would be enhanced upon cooling, as they must according to all scenarios for water at supercooled temperatures. From the present work it is, however, clear that a consistent description of the vdW interaction in AIMD simulations provides the key to tuning such a balance.

VI. ACKNOWLEDGMENTS

The authors would like to thank the Lundbeck foundation for sponsoring the Center for Atomic-scale Materials Design (CAMD) and the Danish Center for Scientific Computing for providing computational resources. The authors would also like to thank the Department of Energy, Basic Energy Sciences, National Science Foundation (CHE-0809324), Denmark-America Foundation and the Swedish Research Council.

¹ Ph. Wernet, D. Nordlund, U. Bergmann, M. Cavalleri, M. Odelius, H. Ogasawara, L.Å. Näslund, T.K. Hirsch, L. Ojamäe, P. Glatzel, L.G.M. Pettersson, and A. Nilsson. *Science*, 304:995, 2004.

² J.D. Smith, C.D. Cappa, K.R. Wilson, B.M. Messer, R.C. Cohen, and R.J. Saykally. Energetics of Hydrogen Bond Network Rearrangements in Liquid Water. *Science*, 306:851, 2004.

³ A. Nilsson, Ph. Wernet, D. Nordlund, U. Bergmann, M. Cavalleri, M. Odelius, H. Ogasawara, L.-Å. Näslund, T. K. Hirsch, L. Ojamäe, P. Glatzel, and L. G. M. Pettersson. Comment on Energetics of Hydrogen Bond Network Rearrangements in Liquid Water. *Science*, 308:793a, 2005.

⁴ B. Hetényi, F. De Angelis, P. Giannozzi, and R. Car. Calculation of near-edge x-ray-absorption fine structure at finite temperatures: Spectral signatures of hydrogen bond

breaking in liquid water. *J. Chem. Phys.*, 120:8632, 2004.

⁵ M. Cavalleri, D. Nordlund, M. Odelius, A. Nilsson, and L.G.M. Pettersson. Half or full core-hole in Density Functional Theory X-ray absorption spectrum calculations of water? *Phys. Chem. Chem. Phys.*, 7:2854, 2005.

⁶ D. Kennedy and C. Norman. *Science*, 309:75, 2005.

⁷ M. Odelius, M. Cavalleri, A. Nilsson, and L.G.M. Pettersson. The X-ray Absorption Spectrum of Liquid Water from Molecular Dynamics Simulations: Asymmetric Model. *Phys. Rev. B*, 73:024205, 2006.

⁸ D. Prendergast and G. Galli. X-ray absorption spectra of water from first principles calculations. *Phys. Rev. Lett.*, 96:215502, 2006.

⁹ H.S. Lee and M.E. Tuckerman. *J. Chem. Phys.*, 125:154507, 2006.

¹⁰ M. Leetmaa, K. T. Wikfeldt, M. P. Ljungberg,

- M. Odelius, J. Swenson, A. Nilsson, and L. G. M. Pettersson. Diffraction and IR/Raman data do not prove tetrahedral water. *J. Chem. Phys.*, 129:084502, 2008.
- ¹¹ O. Fuchs, M. Zharnikov, L. Weinhardt, M. Blum, M. Weigand, Y. Zubavichus, M. Bär, F. Maier, JD Denlinger, C. Heske, et al. Isotope and temperature effects in liquid water probed by X-ray absorption and resonant X-ray emission spectroscopy. *Phys. Rev. Lett.*, 100(2):27801, 2008.
- ¹² T. Tokushima, Y. Harada, O. Takahashi, Y. Senba, H. Ohashi, L. G. M. Pettersson, A. Nilsson, and S. Shin. High resolution X-ray emission spectroscopy of liquid water: The observation of two structural motifs. *Chem. Phys. Lett.*, 460(4-6):387–400, 2008.
- ¹³ L.G.M. Pettersson, T. Tokushima, Y. Harada, O. Takahashi, S. Shin, and A. Nilsson. Comment on Isotope and Temperature Effects in Liquid Water Probed by X-ray Absorption and Resonant X-ray Emission Spectroscopy. *Phys. Rev. Letters*, 100:249801, 2008.
- ¹⁴ K.T. Wikfeldt, M. Leetmaa, M.P. Ljungberg, A. Nilsson, and L.G.M. Pettersson. *J. Phys. Chem. B*, 113:6246, 2009.
- ¹⁵ C. Huang, K. T. Wikfeldt, T. Tokushima, D. Nordlund, Y. Harada, U. Bergmann, M. Niebuhr, T.M. Weiss, Y. Horikawa, M. Leetmaa, M.P. Ljungberg, O. Takahashi, A. Lenz, L. Ojamäe, A.P. Lyubartsev, S. Shin, L.G.M. Pettersson, and A. Nilsson. The inhomogeneous structure of water at ambient conditions. *Proc. Natl. Acad. Sci. USA*, 106:15214, 2009.
- ¹⁶ F. Mallamace, M. Broccio, C. Corsaro, A. Faraone, D. Majolino, V. Venuti, L. Liu, C.-Y. Mou, and S.-H. Chen. *Proc. Natl. Acad. Sci. USA*, 104:424–428, 2007.
- ¹⁷ M. Odelius. Molecular dynamics simulations of fine structure in oxygen K-edge x-ray emission spectra of liquid water and ice. *Phys. Rev. B*, 79(14):144204, 2009.
- ¹⁸ A.K. Soper, J. Teixeira, and T. Head-Gordon. Is ambient water inhomogeneous on the nanometer-length scale? *Proc. Natl. Acad. Sci. USA*, 107:E44, 2010.
- ¹⁹ C. Huang, K. T. Wikfeldt, T. Tokushima, D. Nordlund, Y. Harada, U. Bergmann, M. Niebuhr, T.M. Weiss, Y. Horikawa, M. Leetmaa, M.P. Ljungberg, O. Takahashi, A. Lenz, L. Ojamäe, A.P. Lyubartsev, S. Shin, L.G.M. Pettersson, and A. Nilsson. Reply to Soper "Fluctuations in water around a bimodal distribution of local hydrogen bonded structural motifs". *Proc. Natl. Acad. Sci. USA*, 107:E45, 2010.
- ²⁰ W. Chen, X. Wu, and R. Car. X-Ray Absorption Signatures of the Molecular Environment in Water and Ice. *Phys. Rev. Lett.*, 105:017802, 2010.
- ²¹ G.N.I. Clark, G.L. Hura, J. Teixeira, A.K. Soper, and T. Head-Gordon. Small-angle scattering and the structure of ambient liquid water. *Proc. Natl. Acad. Sci. USA*, 107(32):14002–14007, 2010.
- ²² G. N. I. Clark, C. D. Cappa, J. D. Smith, R. J. Saykally, and T. Head-Gordon. The Structure of Ambient Water. *Mol. Phys.*, 108:1415, 2010.
- ²³ A.K. Soper. Recent Water Myths. *Pure Appl. Chem.*, 82:1855, 2010.
- ²⁴ A. K. Soper. *J. Phys. Condens. Matter*, 17:S3271–S3282, 2005.
- ²⁵ K.T. Wikfeldt, M. Leetmaa, A. Mace, A. Nilsson, and L.G.M. Pettersson. *J. Chem. Phys.*, 132:104513, 2010.
- ²⁶ S.V. Lishchuk, N.P. Malomuzh, and P.V. Makhlaichuk. Why thermodynamic properties of normal and heavy water are similar to those of argon-like liquids? *Phys. Lett. A*, 374:2084, 2010.
- ²⁷ P.G. Debenedetti. Supercooled and glassy water. *J. Phys.: Condens. Matter*, 15:R1669, 2003.
- ²⁸ H.E. Stanley, S.V. Buldyrev, G. Franzese, P. Kumar, F. Mallamace, M.G. Mazza, K. Stokely, and L. Xu. *J. Phys.: Condens. Matter*, 22:284101, 2010.
- ²⁹ F. Mallamace. *Proc. Natl. Acad. Sci. USA*, 106:15097, 2009.
- ³⁰ R.J. Speedy. *J. Phys. Chem.*, 86:3002, 1982.
- ³¹ H.E. Stanley and J. Teixeira. *J. Chem. Phys.*, 73:3404, 1980.
- ³² P.H. Poole, F. Sciortino, U. Essmann, and H.E. Stanley. *Nature*, 360:324–328, 1992.
- ³³ K. Stokely, M.G. Mazza, H.E. Stanley, and G. Franzese. Effect of hydrogen bond cooperativity on the behavior of water. *Proc. Natl. Acad. Sci. USA*, 107(4):1301, 2010.
- ³⁴ R.J. Speedy and C.A. Angell. Isothermal compressibility of supercooled water and evidence for a thermodynamic singularity at -45 C. *J. Chem. Phys.*, 65:851, 1976.
- ³⁵ O. Mishima and H. E. Stanley. *Nature*, 396:329, 1998.
- ³⁶ P.H. Poole, F. Sciortino, T. Grande, H.E. Stanley, and C.A. Angell. *Phys. Rev. Lett.*, 73:1632, 1994.
- ³⁷ S.S. Borick, P.G. Debenedetti, and S. Sastry. *J. Phys. Chem.*, 99:3781, 1995.
- ³⁸ I. Brovchenko and A. Oleinikova. *J. Chem. Phys.*, 124:164505, 2006.
- ³⁹ S. Sastry, P. G. Debenedetti, F. Sciortino, and H. E. Stanley. Singularity-Free Interpretation of the Thermodynamics of Supercooled Water. *Phys. Rev. E*, 53:6144, 1996.
- ⁴⁰ C. A. Angell. Insights into Phases of Liquid Water from Study of Its Unusual Glass-Forming Properties. *Science*, 319:582, 2008.
- ⁴¹ R. J. Speedy. Stability-limit conjecture. An interpretation of the properties of water. *J. Phys. Chem.*, 86:982, 1982.
- ⁴² R. Car and M. Parrinello. *Phys. Rev. Lett.*, 55:2471, 1985.
- ⁴³ V. Molinero and E.B. Moore. Water Modeled As an Intermediate Element between Carbon and Silicon. *J. Phys. Chem. B*, 113(13):4008–4016, 2008.
- ⁴⁴ A.K. Soper. *J. Phys. Condens. Matter*, 19:335206, 2007.
- ⁴⁵ L. Fu, A. Bienenstock, and S. Brennan. *J. Chem. Phys.*, 131:234702, 2009.
- ⁴⁶ J. Neuefeind, C.J. Benmore, J.K.R. Weber, and D. Paschek. More accurate X-ray scattering data of deeply supercooled bulk liquid water. *Mol. Phys.*, XX:XX, 2010.
- ⁴⁷ E.B. Moore and V. Molinero. Growing correlation length in supercooled water. *J. Chem. Phys.*, 130:244505, 2009.
- ⁴⁸ A.K. Soper. *Chem. Phys.*, 258:121, 2000.
- ⁴⁹ G. Hura, J.M. Sorenson, R.M. Glaeser, and T. Head-Gordon. *J. Chem. Phys.*, 113:9140, 2000.
- ⁵⁰ D. Paschek, A. Rüppert, and A. Geiger. Thermodynamic and Structural Characterization of the Transformation from a Metastable Low-Density to a Very High-Density Form of Supercooled TIP4P- Ew Model Water. *ChemPhysChem*, 9(18):2737–2741, 2008.
- ⁵¹ I. Brovchenko, A. Geiger, and A. Oleinikova. Liquid-liquid phase transitions in supercooled water studied by computer simulations of various water models. *J. Chem. Phys.*, 123:044515, 2005.
- ⁵² C.T. Lee, W.T. Yang, and R.G. Parr. *Phys. Rev. B*, 37(2):785, 1988.
- ⁵³ J.P. Perdew, K. Burke, and M. Ernzerhof. *Phys. Rev. Lett.*, 77:3865, 1996.
- ⁵⁴ J.C. Grossman, E. Schwegler, E.W. Draeger, F. Gygi, and

- G. Galli. *J. Chem. Phys.*, 120:300, 2004.
- ⁵⁵ I.F.W. Kuo, C.J. Mundy, M.J. McGrath, J.I. Siepmann, J. VandeVondele, M. Sprik, J. Hutter, B. Chen, M.L. Klein, F. Mohamed, M. Krack, and M. Parrinello. *J. Phys. Chem. B*, 108:12990, 2004.
 - ⁵⁶ P.H.L. Sit and N. Marzari. *J. Chem. Phys.*, 122:204510, 2005.
 - ⁵⁷ J. VandeVondele, F. Mohamed, M. Krack, J. Hutter, M. Sprik, and M. Parrinello. *J. Chem. Phys.*, 122:014515, 2005.
 - ⁵⁸ T. Todorova, A.P. Seitsonen, J. Hutter, I.F.W. Kuo, and C.J. Mundy. *J. Phys. Chem. B*, 110:3685, 2006.
 - ⁵⁹ S. Yoo, X. C. Zeng, and S. S. Xantheas. On the phase diagram of water with density functional theory potentials: The melting temperature of ice i_h with the perdew–burke–ernzerhof and becke–lee–yang–parr functionals. *J. Chem. Phys.*, 130(22):221102, 2009.
 - ⁶⁰ J. Ireta, J. Neugebauer, and M. Scheffler. *J. Phys. Chem. A*, 108:5692, 2004.
 - ⁶¹ B. Santra, A. Michaelides, M. Fuchs, A. Tkatchenko, C. Filippi, and M. Scheffler. *J. Chem. Phys.*, 129:194111, 2008.
 - ⁶² C.H. Cho, S. Singh, and G.W. Robinson. *J. Chem. Phys.*, 107:7979, 1997.
 - ⁶³ R. Schmid. *Monatsh. Chem.*, 132:1295, 2001.
 - ⁶⁴ A. Michaelides. Private communication.
 - ⁶⁵ S. Kristyan and P. Pulay. *Chem. Phys. Lett.*, 229:175, 1994.
 - ⁶⁶ R.M. Lynden-Bell and P.G. Debenedetti. *J. Phys. Chem. B*, 109:6527, 2005.
 - ⁶⁷ I.C. Lin, A.P. Seitsonen, M.D. Coutinho-Neto, I. Tavernelli, and U. Rothlisberger. *J. Phys. Chem. B*, 113:1127, 2009.
 - ⁶⁸ F.A. Gianturco, F. Paesani, M.F. Laranjeira, V. Vasilenko, and M.A. Cunha. Intermolecular forces from density functional theory. III. A multiproperty analysis for the $\text{Ar}(^1\text{S})\text{-CO}(^1\Sigma)$ interaction. *J. Chem. Phys.*, 110:7832, 1999.
 - ⁶⁹ S. Grimme. *J. Comput. Chem.*, 25:1463, 2004.
 - ⁷⁰ R.W. Williams and D. Malhotra. *Chem. Phys.*, 327:54, 2006.
 - ⁷¹ M. Dion, H. Rydberg, E. Schröder, D.C. Langreth, and B.I. Lundqvist. *Phys. Rev. Lett.*, 92:246401, 2004.
 - ⁷² J. Wang, G. Roman-Perez, J. M. Soler, E. Artacho, and M. V. Fernandez-Serra. Density, structure, and dynamics of water: The effect of van der Waals interactions. *J. Chem. Phys.*, 134:024516, 2011.
 - ⁷³ A.K. Kelkkanen, B.I. Lundqvist, and J.K. Nørskov. *J. Chem. Phys.*, 131:046102, 2009.
 - ⁷⁴ A. Gulans, M.J. Puska, and R.M. Nieminen. *Phys. Rev. B*, 79(20):201105, 2009.
 - ⁷⁵ D.C. Langreth, B.I. Lundqvist, S.D. Chakarova-Kack, V.R. Cooper, M. Dion, P. Hyldgaard, A. Kelkkanen, J. Kleis, L.Z. Kong, S. Li, P.G. Moses, E. Murray, A. Puzder, H. Rydberg, E. Schröder, and T. Thonhauser. *J. Phys.: Condens. Matter*, 21:084203, 2009.
 - ⁷⁶ A. Puzder, M. Dion, and D.C. Langreth. *J. Chem. Phys.*, 124, 2006.
 - ⁷⁷ E.D. Murray, K. Lee, and D.C. Langreth. *J. Chem. Theory Comput.*, 5:2754, 2009.
 - ⁷⁸ J.P. Perdew and W. Yue. *Phys. Rev. B*, 33:8800, 1986.
 - ⁷⁹ J. Klimes, D.R. Bowler, and A. Michaelides. *J. Phys. Condens. Matter*, 22:022201, 2010.
 - ⁸⁰ V.R. Cooper. *Phys. Rev. B*, 81:161104, 2010.
 - ⁸¹ J. Wellendorff, A. Møgelhøj, V. Petzold, T. Bligaard, K.W. Jacobsen and J.K. Nørskov. to be submitted.
 - ⁸² K. Lee, E.D. Murray, L. Kong, B.I. Lundqvist, and D.C. Langreth. *Phys. Rev. B*, 82:081101, 2010.
 - ⁸³ G. Roman-Perez and J.M. Soler. *Phys. Rev. Lett.*, 103:096102, 2009.
 - ⁸⁴ Y.K. Zhang and W.T. Yang. *Phys. Rev. Lett.*, 80:890, 1998.
 - ⁸⁵ P. Jurecka, J. Sponer, J. Cerny, and P. Hobza. *Phys. Chem. Chem. Phys.*, 8:1985, 2006.
 - ⁸⁶ Y. Wang and J. Perdew. *Phys. Rev. B: Condens. Matter*, 33:8800(R), 1986.
 - ⁸⁷ L.F. Molnar, X. He, B. Wang, and K.M. Merz. *J. Chem. Phys.*, 131:065102, 2009.
 - ⁸⁸ T. Takatani, E.G. Hohenstein, M. Malagoli, M.S. Marshall, and C.D. Sherrill. Basis set consistent revision of the S22 test set of noncovalent interaction energies. *J. Chem. Phys.*, 132:144104, 2010.
 - ⁸⁹ J. Enkovaara, C. Rostgaard, J. J. Mortensen, J. Chen, M. Dulak, L. Ferrighi, J. Gavnholt, C. Glinsvad, V. Haikola, H. A. Hansen, H. H. Kristoffersen, M. Kuisma, A. H. Larsen, L. Lehtovaara, M. Ljungberg, O. Lopez-Acevedo, P. G. Moses, J. Ojanen, T. Olsen, V. Petzold, N. A. Romero, J. Stausholm-Møller, M. Strange, G. A. Tritsarlis, M. Vanin, M. Walter, B. Hammer, H. Hakkinen, G. K. H. Madsen, R. M. Nieminen, J. K. Nørskov, M. Puska, T. T. Rantala, J. Schiøtz, K. S. Thygesen, and K. W. Jacobsen. Electronic structure calculations with GPAW: a real-space implementation of the projector augmented-wave method. *J. Phys.: Cond. Mat.*, 22:253202, 2010.
 - ⁹⁰ L. B. Hansen J. J. Mortensen and K. W. Jacobsen. *Phys. Rev. B*, 71:035109, 2005.
 - ⁹¹ L.A. Curtiss, K. Raghavachari, P.C. Redfern, and J.A. Pople. *J. Chem. Phys.*, 106:1063, 1997.
 - ⁹² J.M. Sorenson, G. Hura, R.M. Glaeser, and T. Head-Gordon. *J. Chem. Phys.*, 113:9149, 2000.
 - ⁹³ T. Head-Gordon and G. Hura. *Chem. Rev.*, 102:2651, 2002.
 - ⁹⁴ R. L. McGreevy and L. Pusztai. *Mol. Simul.*, 1:359, 1988.
 - ⁹⁵ P. Jedlovsky, I. Bako, G. Palinkas, T. Radnai, and A.K. Soper. RMC giving maximally disordered structures. *J. Chem. Phys.*, 105:245, 1996.
 - ⁹⁶ L. Pusztai. Partial pair correlation functions of liquid water. *Phys. Rev. B*, 60(17):11851–11854, 1999.
 - ⁹⁷ S. Myneni, Y. Luo, L.Å. Näslund, M. Cavalleri, L. Ojamäe, H. Ogasawara, A. Pelmenchikov, Ph. Wernet, P. Väterlein, C. Heske, Z. Hussain, L.G.M. Pettersson, and A. Nilsson. Spectroscopic probing of local hydrogen bonding structures in liquid water. *J. Phys.: Condens. Mat.*, 14:L213, 2002.
 - ⁹⁸ P. -L. Chau and A. J. Hardwick. *Mol. Phys.*, 93:511, 1998.
 - ⁹⁹ J.R. Errington and P.G. Debenedetti. Relationship Between Structural Order and the Anomalies of Liquid Water. *Nature*, 409:318, 2001.
 - ¹⁰⁰ G. Ruocco, M. Sampoli, and R. Vallauri. Analysis of the network topology in liquid water and hydrogen sulphide by computer simulation. *J. Chem. Phys.*, 96:6167, 1992.
 - ¹⁰¹ A. Soper and C.J. Benmore. *Phys. Rev. Lett.*, 101:065502, 2008.
 - ¹⁰² C. Huang, T. M. Weiss, D. Nordlund, K. T. Wikfeldt, L. G. M. Pettersson, and A. Nilsson. Increasing correlation length in bulk supercooled H_2O , D_2O , and NaCl solution determined from small angle x-ray scattering. *J. Chem.*

- Phys.*, 133:134504, 2010.
- ¹⁰³ P. Kumar. Breakdown of the StokesEinstein relation in supercooled water. *Proc. Natl. Acad. Sci. USA*, 103:12955–12956, 2006.
 - ¹⁰⁴ L. Xu, F. Mallamace, Z. Yan, F. W. Starr, S. V. Buldyrev, and H. E. Stanley. Appearance of a Fractional Stokes-Einstein Relation in Water and a Structural Interpretation of Its Onset. *Nature Physics*, 5:565–569, 2009.
 - ¹⁰⁵ A.V. Okhulkov, Y.N. Demianets, and Y. E. Gorbaty. *J. Chem. Phys.*, 100:1578, 1994.
 - ¹⁰⁶ J. L. Finney, D. T. Bowron, A. K. Soper, T. Loerting, E. Mayer, and A. Hallbrucker. Structure of a New Dense Amorphous Ice. *Phys. Rev. Lett.*, 89:20553, 2002.
 - ¹⁰⁷ M.M. Koza, B. Geil, K. Winkel, C. Kähler, F. Czeschka, M. Scheuermann, H. Schober, and T. Hansen. Nature of Amorphous Polymorphism of Water. *Phys. Rev. Lett.*, 94:125506, 2005.
 - ¹⁰⁸ M.M. Koza, T. Hansen, R.P. May, and H. Schober. *J. Non-Cryst. Solids*, 352:4988, 2006.
 - ¹⁰⁹ H. Schober, M. Koza, A. Tölle, F. Fujara, C.A. Angell, and R. Böhmer. *Physica B*, 241:897, 1998.
 - ¹¹⁰ C.A. Tulk, C.J. Benmore, J. Utquidi, D.D. Klug, J. Neuefeind, B. Tomberli, and P.A. Egelstaff. *Science*, 297:1320, 2002.
 - ¹¹¹ A. K. Soper and M. A. Ricci. *Phys. Rev. Lett.*, 84:2881, 2000.
 - ¹¹² F. Paesani, S. Iuchi, and G.A. Voth. *J. Chem. Phys.*, 127:074506, 2007.
 - ¹¹³ F. Paesani and G.A. Voth. *J. Phys. Chem. B*, 113:5702, 2009.
 - ¹¹⁴ S. Kaya, S. Yamamoto, N. Huang, J. T. Newberg, H. Bluhm, L. G. M. Pettersson, H. Ogasawara, and A. Nilsson. . *unpublished*.